Journal of Molecular Catalysis B: Enzymatic 122 (2015) 314–322

Contents lists available at ScienceDirect

Journal of Molecular Catalysis B: Enzymatic

journal homepage: www.elsevier.com/locate/molcatb

Piano-stool d^6-rhodium(III) complexes of chelating pyridine-based ligands and their papain bioconjugates for the catalysis of transfer hydrogenation of aryl ketones in aqueous medium

Nathalie Madern[a,b], Nicolas Queyriaux[a,b], Alice Chevalley[a,b], Mahsa Ghasemi[a,b], Orazio Nicolotti[c,d], Ilaria Ciofini[e], Giuseppe Felice Mangiatordi[c,*], Michèle Salmain[a,b,**]

[a] Sorbonne Universités, UPMC Univ Paris 6, UMR 8232, IPCM, F-75005 Paris, France
[b] CNRS, UMR 8232, IPCM, F-75005 Paris, France
[c] Dipartimento di Farmacia—Scienze del Farmaco, Via Orabona, 4, Università di Bari "Aldo Moro", Bari, Italy
[d] Centro Ricerche TIRES, University of Bari "Aldo Moro", Via Amendola 173, I-70126 Bari, Italy
[e] PSL Research University, Chimie ParisTech—CNRS, Institut de Recherche de Chimie Paris, 75005 Paris, France

ARTICLE INFO

Article history:
Received 23 July 2015
Received in revised form 2 October 2015
Accepted 10 October 2015
Available online 22 October 2015

Keywords:
Rhodium
Hydrogenation
Artificial metalloenzyme
Metallocenter assembly
Covalent docking

ABSTRACT

Two half-sandwich d^6-rhodium(III) complexes of the general formula [(η^5-Cp*)Rh(NÑ)Cl]Cl where NÑ is a phenanthroline or a bispyridine methane derivative carrying a thiol-targeting maleimide or chloroacetamide function were synthesized and characterized. Both complexes were able to catalyse the transfer hydrogenation of 2,2,2-trifluoroacetophenone in aqueous medium using formate or phosphite as hydrogen donor. Covalent anchoring of these complexes to the cysteine endoproteinase papain yielded hybrid metalloproteins with transfer hydrogenase properties. Under optimized conditions of pH, hydrogen donor concentration and catalyst load, conversion of substrate was nearly quantitative within 24 h at 40 °C and the (*S*)-enantiomer was obtained preferably albeit with a modest enantiomeric excess of 7–10%. Covalent docking simulations complemented the experimental findings suggesting a molecular rationale for the observed low enantioselectivity. The harmonious use of experimental and theoretical approaches represents an unprecedented starting point for driving the rational design of artificial metalloenzymes built up from papain with higher catalytic efficiency.

1. Introduction

Artificial metalloenzymes are biohybrid species relying on the tight association of a metal-containing species and a biomacromolecule (peptide, protein, DNA). Their development is motivated by the complementary properties of metal catalysts and enzymes and the ability of these hybrid catalysts to operate in environmentally friendly conditions [1,2]. Incorporation of nonnative metal cofactors into proteins has been rationalized into three main strategies: covalent, supramolecular and dative anchoring [3,4]. Each of these strategies has its pros and cons and the supramolecular assembling approach has provided the most efficient catalysts in terms on activity and selectivity so far [5]. Nonetheless, the covalent anchoring approach still remains very attractive because of its simplicity, especially when the protein host contains a reactive residue that can be specifically targeted and whose location is appropriate [6]. These features are met in the case of papain (E.C. 3.4.22.2), a cysteine endoproteinase isolated from *Carica papaya* [7]. It is found in papaya latex along with three other homologous enzymes, namely chymopapain, glycyl endopeptidase (GEP) and caricain [8]. Papain consists of a single polypeptidic chain of 212 aminoacids. Its active site forms a 15 × 25 Å groove between its two domains [9]. Two aminoacids are essential for the activity of papain, namely Cys25 and His159. The thiolate group of Cys25 is known to be highly nucleophilic because of its location and its chemical modification invariably leads to loss of hydrolytic activity, providing a convenient means to monitor the reaction between papain and thiol-targeted reagents [10]. These properties provided a starting point for Kaiser's early concept of chemical mutation of proteins [11–15] and later on for the design of artificial metalloenzymes by covalent anchoring of metal complexes [16–24].

* Corresponding author.
** Corresponding author at: Sorbonne Universités, UPMC Univ Paris 6, UMR 8232, IPCM, F-75005 Paris, France.
E-mail addresses: giuseppe.mangiatordi@uniba.it (G.F. Mangiatordi), michele.salmain@upmc.fr (M. Salmain).

http://dx.doi.org/10.1016/j.molcatb.2015.10.007
1381-1177/

To confer papain with transfer hydrogenase activity, we had previously designed and synthesized monocationic (arene)Ru^{II} and (Cp*)Rh^{III} complexes of 2,2′-dipyridylamine carrying a thiol-targeted maleimide function appended to the central nitrogen atom via an butyl or pentyl spacer [16]. Covalent anchoring of these complexes to papain was achieved and the metallopapains were shown to display transfer hydrogenase activity on a model substrate. The Rh^{III} adducts were by far the most active as quantitative conversion was reached within 60 h at 40 °C and neutral pH in the presence of 1 mol% metallopapain. Disappointingly, the enantiomeric excess reached 15% at best in favour of the (*R*)-enantiomer [22]. Notably, asymmetric transfer hydrogenation (ATH) is a powerful means to access secondary chiral alcohols and amines from ketones and imines, respectively [25,26]. Numerous piano-stool d^6 $ruthenium^{II}$, $rhodium^{III}$ and $iridium^{III}$ complexes including chiral diamine ligands catalyse the ATH of ketones in neat water using formate as hydrogen donor [27–41]. Some half-sandwich polypyridine-type $ruthenium^{II}$, $rhodium^{III}$ and $iridium^{III}$ complexes display the same reactivity [42–51]. In both cases, the reaction mechanism involves the transient formation of a metal-hydride species resulting from a β-elimination process [34,52]. Artificial transfer hydrogenases resulting from the supramolecular anchoring of biotinylated piano-stool diamine complexes to (strept) avidin have been shown to catalyse the ATH of ketones and imines with high conversion and enantioselectivity [53–57]. Also, achiral half-sandwich Rh^{III} complexes derived from fatty acids catalysed the ATH of the benchmark substrate 2,2,2-trifluoroacetophenone (TFACP) with up to 32% ee in the presence of bovine β-lactoglobulin [58,59].

In this study, we report the synthesis of two new (Cp*)Rh^{III} complexes containing a polypyridine chelating ligand carrying a thiol-targeted chloroacetamide or maleimide function without spacer so as to shorten the distance between the metal centre and the second coordination sphere and restrict the number of conformations of the metal complex when bound to the protein. Their covalent anchoring to papain and the catalytic activity of the complexes and the metallopapain adducts in the hydrogenation of TFACP was assessed. In parallel, molecular modelling studies combining quantum mechanics (QM) calculations and covalent docking simulations allowed us to obtain valuable insights into the posing of the anchored metal complexes within the protein-binding site. It is worth noting that molecular docking, a computational technique commonly employed for drug design, is today considered a valuable tool to speed up the design process of artificial metalloenzymes, as recently pointed out by Robles et al. [60]. The theoretical outcomes, consistent with the observed ee's as well as with X-ray data obtained for a similar metal–complex anchored to papain, unveiled the molecular rationale ruling the observed disappointing enantioselectivity. These outcomes are discussed in the perspective of providing rational pathways to design more efficient piano-stool d^6-$rhodium^{III}$ cofactors.

2. Experimental

2.1. General

Solvents were dried and distilled by standard procedures and all reactions and synthetic manipulations were performed under an inert atmosphere of argon using standard Schlenk and vacuum-line techniques. ^1H and ^{13}C NMR spectra were recorded on a 300 and 400 MHz FT-spectrometers (Bruker). Crude papain (**cPAP**) was purchased from Sigma (reference 76220). Other chemicals were purchased from Aldrich or Alfa-Aesar and used as received. 2-chloro-*N*-(1,10-phenanthrolin-5-yl) acetamide **1** [61] and di(2-pyridyl) methylamine **2** [62] were synthesized according to literature procedures. ATR-IR spectra were measured on FTIR-4100 spectrometer (Jasco). Uv–visible spectra were recorded on a Cary 50 spectrometer (Varian). Circular dichroism spectra were recorded at 20 ± 0.1 °C on a J-815CD spectrometer (Jasco) applying the following parameters: scan speed 50 nm/min, band width 1 nm, data pitch 0.5 nm, 3 scans. HPLC was carried out on a System Gold (Beckman Coulter). Reaction mixtures were analysed on a 150 × 2 mm reverse-phase column (Jupiter Proteo, Phenomenex) under isocratic conditions (H_2O/MeCN 60:40 at 0.2 ml/min) or on a 200 × 4 mm chiral column (Nucleodex β-CD, Macherey-Nagel) under isocratic conditions (H_2O/MeCN 60:40 at 0.4 ml/min). LC-ESI–MS spectra were recorded on a 6210 LC–TOF mass spectrometer (Agilent) equipped with a protein trap (Zorbax 300SB-C8, 5 um, 5 × 0.3 mm) and RP-HPLC column (Vydac C4 5 um, 300 Å, 50 × 0.5 mm). A linear gradient from 5 to 95% of MeCN/H_2O/TFA 95:5:0.03 in H_2O/TFA 100:0.03 was applied in 15 min. Affinity-purified papain (**afPAP**) was obtained from crude papain by affinity chromatography as previously described [63]. The enzymatic activity of crude papain was measured on the chromogenic substrates *N*-alpha-benzyloxycarbonyl-glycyl-*p*-nitrophenylester ZGlyONp (Fluka), *N*-alpha-benzoyl-DL-arginine 4-nitroanilide BAPNa (Sigma) and L-pyrogLutamyL-L-phenylalanyl-L-leucine-*p*-nitroanilide PFLNa (Bachem) in 100 mM phosphate buffer pH 6.5, 30 mM KCl, 0.1 mM EDTA containing 10% DMSO (BAPNa and PFLNa) or MeCN (ZGlyONp) (v/v). The protein concentration was determined by absorbance measurement at 280 nm taking ϵ = 46,000 M^{-1} cm^{-1} for **cPAP** and 57,600 M^{-1} cm^{-1} for **afPAP**. Alternatively, protein concentration was measured by the Bradford assay. Thiol concentration was assayed at 324 nm after reaction with 4,4′-dithiodipyridine [64].

2.2. Synthesis

2.2.1. 1-(di(pyridin-2-yl) methyl)-1H-pyrrole-2,5-dione **3**

A solution of **2** (500 mg, 2.7 mmol, 1 eq) in dry toluene (1 ml) was added dropwise to a stirred solution of maleic anhydride (265 mg, 2.7 mmol, 1 eq) in dry toluene (5 ml) at room temperature. During the addition, an exothermic reaction occurred with instantaneous formation of white precipitates. After the addition was complete, the resulting suspension was stirred for 1 h and then $ZnCl_2$ (362 mg, 2.7 mmol, 1 eq) was added in one portion. While the resulting reaction mixture was heated (80 °C), a solution of HMDS (834 μL, 4 mmol, 1.5 eq) in dry toluene (1 ml) was added slowly over a period of 10 min, and then the mixture was refluxed for 1 h. The reaction mixture was cooled to room temperature and poured into saturated NH_4Cl. The aqueous phase was extracted with ethyl acetate. The organic extract was washed with saturated brine and dried over anhydrous Na_2SO_4. The solution was concentrated under reduced pressure to leave the residue, which was purified by silica filtration (silica gel, petroleum ether/EtOAc 8:2) to afford compound **3** (612 mg, 74%) as a colorless solid. ^1H NMR (300 MHz, $CDCl_3$) ∂ in ppm 8.65–8.55 (m, 2H, H1), 7.68 (td, 2H, *J* = 7.8, 1.8 Hz, H2 or H3), 7.34–7.20 (m, 4H, H2 or H3 & H4), 6.77 (s, 2H, H8), 6.70 (s, 1H, H6). ^{13}C NMR (75 MHz, $CDCl_3$) ∂ in ppm 170.6 (C7), 158.5 (C5), 149.4 (C1), 136.9 (C4 or C8), 134.5 (C4 or C8), 123.6 (C3 or C2), 123.0 (C2 or C3), 60.6 (C6). MS (CI/NH_3): *m*/*z* 266.02 [MH^+].

2.2.2. [(η^5-Cp*)Rh(2-chloro-N-(1,10-phenanthrolin-5-yl) acetamide)Cl]Cl **1-Rh**

[Cp*RhCl(μ-Cl)]$_2$ (0.1 g, 0.162 mmol) was introduced into a Schlenk tube followed by DCM (10 ml) and **1** (0.324 mmol, 88 mg). After 3 h, the solvent was removed by evaporation under reduced pressure and the residue was washed three times with 10 ml diethyl ether. Compound [(η^5-Cp*)Rh(2-chloro-*N*-(1,10-phenanthrolin-5-yl) acetamide)Cl]Cl **1-Rh** was obtained as a red solid (36%) after drying under high vacuum. ^1H NMR (300 MHz, $CDCl_3$) δ in ppm 12.20 (s, 1H, NH), 9.99 (d, *J* = 8.2 Hz,

1H, H4), 9.06 (d, J = 54.7 Hz, 1H, H2), 8.98 (d, J = 4.8 Hz, 1H, H9), 8.71 (s, 1H, H6), 8.44 (d, J = 7.8 Hz, 1H, H7), 8.14 (dd, 1H, J = 7.9, 5.5 Hz, H8), 7.87 (dd, 1H, J = 7.5, 5.5 Hz, H3), 4.91 (d, 1H, J = 14.1 Hz, H13a), 4.84 (d, 1H, J = 14.1 Hz, H13b), 1.74 (s, 15H, 5Me(Cp)). ^{13}C NMR (75 MHz, DMSO-d6) δ in ppm 167.8 (C12), 151.4 (C2), 149.9 (C9), 145.5 (C1a), 142.9 (C10a), 138.5 (C7), 137.7 (C4), 134.6 (C5), 130.7 (C6a), 127.1 (C4a), 126.9 (C3), 126.8 (C8), 118.5 (C6), 97.0 (Cp*), 44.3 (C13), 9.4 (Me). IR ν in cm^{-1}: 1705 (amide), 1590 (amide), 1023 (Cp*), 727 (aromatic). Uv (H_2O) λ in nm (ϵ in M^{-1} cm^{-1}) 277 (20,500), 353sh (2900). HR-MS: calcd for $C_{24}H_{25}N_3OCl_2Rh^+$ 544.04242, found 544.04254.

2.2.3. [(η^5-Cp*)Rh(1-(di(pyridin-2-yl) methyl)-1H-pyrrole-2,5-dione)Cl]Cl ***3-Rh***

To a stirred solution of **3** (300 mg, 1.1 mmol) in dry CH_2Cl_2 (5 ml) was added [Cp*Rh(μ-Cl)Cl]$_2$ (283 mg, 0.55 mmol). The mixture was stirred at room temperature for 16 h. Solvent was evaporated under reduced pressure and diethyl ether was added. The yellow crystals were filtered and washed with diethyl ether. Compound [(η^5-Cp*)Rh(1-(di(pyridin-2-yl) methyl)-1H-pyrrole-2,5-dione)Cl]Cl **3-Rh** was obtained as a yellow–orange solid (96%). ^{1}H NMR (300 MHz, DMSO-d^6) ∂ in ppm (mixture of chloro and aqua complexes) 8.93 and 8.71 (d, J = 5.1 or 4.8 Hz, 2H, H1), 8.09 and 7.93 (t or td, J = 7.2 or 8.1 and 1.5 Hz, 2H, H2), 7.64 and 7.38 (d, J = 7.8 or 8.1 Hz, 2H, H4), 7.57 and 7.49 (t, J = 6.3 or 5.7 Hz, 2H, H3) 7.27 and 7.26 (s, 2H, H8), 7.00 and 6.80 (s, 1H, H6), 1.65 (s, 15H, Cp*). Uv (H_2O) λ in nm (ϵ in M^{-1} cm^{-1}) 253sh (10,200), 351 (2100). MS (ESI) m/z 538.4 [M$^+$].

2.3. Kinetics of inactivation of crude papain by ***1-Rh*** or ***3-Rh***

A solution of crude papain (2 mg solid/ml in 20 mM phosphate buffer pH 7.0; [thiol] = 0.11 mM) was treated with excess **1-Rh** (1 mM). Aliquots of the solution were periodically assayed for their enzymatic activity on BAPNa, PFLNa and ZGlyONp. A solution of crude papain (10 mg solid/ml in water; 5 ml) was first submitted to gel filtration to remove low molecular weight thiols contained in the commercial sample. The resulting protein sample was diluted to 93 μg/ml in PBS ([thiol] = 3 μM) and treated with excess **3-Rh** (100 μM). Aliquots of the solution were periodically assayed for their enzymatic activity on ZGlyONp.

2.4. Cation exchange chromatography of ***cPAP-1-Rh***

A solution of crude papain (10 mg solid/ml in 20 mM phosphate, 0.4 M NaCl pH 7; [thiol] = 0.56 mM) was treated with **1-Rh** (0.7 mM). After 24 h, the solution was passed on a gel filtration column (Hiprep D-salt 26/10) using 150 mM acetate pH 5 as eluent. The protein sample was applied to a Mono S 5/5 cation exchange column (GE Healthcare) equilibrated with 150 mM acetate pH 5. Proteins were eluted using a linear gradient of NaCl (31 mM/ml) at a flow rate of 0.7 ml/min. Fractions of 0.35 ml were collected and assayed for enzymatic activity on ZGlyONp.

2.5. Assembling of crude papain and ***1-Rh*** or ***3-Rh***

A solution of crude papain (10 mg solid/ml in 20 mM phosphate, 0.4 M NaCl pH 7; [thiol] = 0.56 mM) was treated with **1-Rh** (0.64 mM). After 30 h, NEM (1.28 mM) was added and the mixture incubated for another 17 h to block residual enzymatic activity. Unreacted complex and NEM were removed by diafiltration with water in a stirred cell (Amicon) to yield **cPAP-1-Rh**. The same procedure was applied with a slight excess of **3-Rh** over thiol (0.83 mM, 1.5 eq.) while omitting the NEM step to yield **cPAP-3-Rh**.

2.6. Kinetics of inactivation and assembling of affinity-purified papain to 1-Rh

A solution of affinity-purified papain (6 μM in 20 mM phosphate, 0.4 M NaCl pH 7) was treated with **1-Rh** (100 μM). Aliquots of the solution were periodically assayed for their enzymatic activity on PFLNa over a period of 3 h. After 18 h, the solution was concentrated by ultrafiltration in a 50 ml stirred cell (Amicon) and excess complex was separated from the protein by gel filtration (Hiprep 26/10 desalting, GE Healthcare) using 150 mM NaCl as eluent. The resulting protein solution was diluted with 2 volumes of water and concentrated by ultrafiltration to yield **afPAP-1-Rh**.

2.7. Transfer hydrogenation of TFACP

Test mixtures (1 ml) containing TFACP (5 or 10 mM), hydrogen donor and catalyst in water were incubated at 40 °C in a dry bath. Aliquots (10 μl) were retrieved periodically and analysed by reverse phase or chiral HPLC.

2.8. Modelling studies

In order to evaluate the metal complex posing in the protein-binding site, covalent docking was carried out on both compounds **1-Rh** and **3-Rh**. The complexes were docked considering only their hydride forms, which are the catalytically active species. Being chiral at the metal centre, both the enantiomers of **1-Rh** were considered (hereafter referred to as **1-Rh(R)** and **1-Rh(S)**) though **1-Rh** is expected to racemize very quickly because of the lability of the chloride ligand. As a first step, the Restrained ElectroStatic Potential (RESP) approach [65] was applied to derive accurate atomic charges to be employed for docking simulations. Compounds were optimized at the Density Functional Theory level using the hybrid B3LYP functional [66]. All atoms were described using a double zeta valence basis set (6–31+G(d,p)) except for Rhodium, described by an effective core potential and corresponding valence basis set. Molecular electrostatic potential (MEP) was then computed on these structures at B3LYP level of theory using a smaller basis set (6–31G(d)). Finally, the charge values were fitted in order to reproduce the computed MEPs. All these calculations were performed with the Gaussian 09 [67] package apart from the charges fitting performed using Antechamber [68], a freely accessible program that is part of AmberTools [69]. Covalent docking studies were performed on the X-ray crystal structure of papain (PDB code: 9PAP [70], resolution 1.65 Å). Protein structure was prepared using the Protein Preparation wizard [71] available from Schrodinger Suite v2014-4 [72]. The resulting file was used for docking simulations performed using the Covalent Docking protocol, enclosed in the Schrodinger Suite [72]. This protocol allows predicting whether compounds can covalently bind a given receptor and, in case, which pose is the most suitable. Following such a protocol, Cys25 was first mutated to alanine, in order to avoid a possible influence of its side chain conformation on the protein-compound association. Docking simulations were then performed using Grid-based Ligand Docking with Energetics (GLIDE v6.5) software [73] enclosed in the Schrodinger Suite [72]. Distance constrains were applied between residue in position 25 and the reactive group of the considered metal–complex. Furthermore, a preliminary minimization of the protein residues close to the docked compounds (distance cut-off = 5 Å) was carried out before selecting suitable docking poses. Subsequently, the Cys25 side chain was restored and its suitable poses explored in the presence of the bound metal-complex. Finally, the covalent bond was formed and both metal-complex and Cys25 were minimized to reduce strain. The described covalent docking protocol was performed using the default Force Field OPLS_2005 [74] except for the atomic charges, which were derived

following the RESP protocol, as described above. A cubic grid having an edge of 30 Å centred on the centroid of residues Cys25, Asp158 and Asn64, and all the default setting for covalent docking simulations were used.

3. Results and discussion

3.1. Synthesis

The chloroacetamide Rh^{III} complex **1-Rh** was synthesized in 2 steps from 5-amino-1,10-phenanthroline (Scheme 1). Its amino group was firstly acetylated with chloroacetyl chloride according to a published procedure [61] then complexation was achieved by reaction of $[Cp^*Rh(\mu\text{-}Cl)Cl]_2$ in DCM. **1-Rh** was characterized by ^1H and ^{13}C NMR. The 7 protons of the polycyclic system were non equivalent because of the dissymmetrical nature of the molecule. Their assignment was done thanks to 2D NMR experiments (COSY, HSQC and HMBC). Interestingly, the two protons H13 were diastereotopic with a geminal coupling constant of 14 Hz because of the chirality at the metal center.

The maleimide Rh^{III} complex **3-Rh** was synthesized in three steps for the commercially available oxime (Scheme 2). The oxime was first converted into di(2-pyridyl) methylamine **2** by reduction in the presence of ammonia and zinc powder according to a previously published procedure [62]. Treatment of the amine with maleic anhydride afforded an intermediate amide. Dehydration to the maleimide attempted in the classical way with acetic anhydride gave maleimide **3** with 26% yield. This yield was increased to 80% by using $ZnCl_2$ and HMDS in toluene at reflux [75]. Finally **3-Rh** was obtained as above and its molecular structure confirmed by ^1H NMR analysis. Both metal complexes are soluble in polar solvents including water where they rapidly hydrolyse to the dicationic aqua complexes.

3.2. Covalent assembling of *1-Rh* and *3-Rh* to papain

Complexes **1-Rh** and **3-Rh** were covalently anchored to papain from 2 different sources, i.e. commercial papain (further called crude papain or **cPAP**) which is in fact lyophilized papaya latex containing all 4 cysteine endoproteinases (and an appreciable amount of low molecular weight thiols) and pure papain (**afPAP**) obtained by affinity chromatography of the commercial sample according to a literature procedure [63]. By analogy with the previously reported reactions of α-chloroacetamides and maleimides with papain [7,76,77], chemical modification of the active site cysteine residue of papain and the 3 other cysteine endoproteinases by **1-Rh** and **3-Rh** should lead to the loss of their catalytic activity. Therefore, the hydrolytic activity of a mixture of **cPAP** and **1-Rh** (in excess with respect to thiol content) was periodically measured on 3 different chromogenic substrates, namely BAPNa, PFLNa, and ZGlyONp (Fig. 1). Papain, caricain and chymopapain have rather broad specificities (aromatic residue at the P2 position is preferred for papain [9]) and catalyse the hydrolysis of PFLNa, BAPNa and ZGlyONp. Conversely, GEP displays a narrow specificity for substrates including a glycyl residue at the P1 position and is therefore only active on ZGlyONp [78].

Time-course plots of residual activity followed a different trend depending on the substrate. The enzymatic activity of the mixture of **cPAP** and **1-Rh** on PFLNa decreased rapidly up to complete inactivation in ca. 50 min. The activity on BAPNa decreased more slowly but complete inactivation was reached within 300 min. For ZGlyONp, activity decreased too but reached a plateau at ca. 40% (i.e. 60% inhibition) after ca. 3 h. It clearly highlights some differences in the reactivity of **1-Rh** towards the individual cysteine endoproteinases of the crude papain sample. A mixture of **cPAP** and **1-Rh** was submitted to gel desalting to remove unreacted complex followed by cation exchange chromatography to separate the individual cysteine endoproteinases. The resulting chromatogram (Fig. S1) displayed 4 major peaks in agreement with the literature [79,80]. The first (I) and last peaks (IV) were readily identified as papain and caricain, respectively while the less well resolved second and third peaks (II and III) were identified as chymopapain and glycyl endopeptidase. Only peak III (v = 21 ml) showed some activity on ZGlyONp. These experimental data, taken together, suggest that **1-Rh** is unable to inactivate GEP. This behaviour of **1-Rh** is consistent with the poor inhibiting properties of both iodoacetate and iodoacetamide towards GEP [81].

Table 1
Rh/protein ratios of the metallopapains.

Complex	**1-Rh**	**3-Rh**
Crude papain	1.5 ± 0.25[a]	0.9 ± 0.1[b]
Affinity-purified papain	1.2 ± 0.2[b]	n.d.

[a] Protein concentration determined by the Bradford assay.
[b] Protein concentration determined at 280 nm.

In a similar fashion, gradual loss of activity of a mixture of **afPAP** and **1-Rh** in excess was observed on PFLNa and the enzyme was fully inactivated after 18 h. Semi-logarithmic plot of PFLNa hydrolysis rate vs. time was linear (Fig. S2) and gave the pseudo-first rate constant of inactivation k_{obs} of 0.004 min^{-1} and the second order rate constant $k_2 = k_{obs}/[\mathbf{1\text{-}Rh}] = 40\ M^{-1}\ min^{-1}$. This value is ten times smaller than those determined for previously reported organometallic chloroacetamide derivatives [17,77] and also much smaller than that of the archetypal irreversible inhibitor TPCK whose second order rate constant is equal to 1200 $M^{-1}\ min^{-1}$ [17].

Reaction of crude papain with excess **3-Rh** was performed with a protein sample devoid of low molecular weight thiols. Rapid loss of activity on ZGlyONp was observed (20% activity remaining after 20 min, Fig. 1) but the semi-logarithmic plot of activity vs. time was nonlinear as depicted in the inset of Fig. 1. This trend reflects the heterogeneous character of crude papain and the fact that the 4 cysteine endoproteinases may be inhibited by **3-Rh** at different rates depending on the relative accessibility of the active site cysteine residue in each enzyme.

Both **1-Rh** and **3-Rh** displayed absorption features in the near-uv range, in particular a band around 350 nm (Figs. S3 and S4). Accordingly, bioconjugates **cPAP-1-Rh, afPAP-1-Rh** and **cPAP-3-Rh** also displayed absorption around 350 nm owing to the metal complex as well as a maximum of absorption at 280 nm typical of proteins (Figs. S3 and S4). The Rh content of the metallopapains was estimated from the absorbance at 350 nm ($\epsilon^{350}(\mathbf{1\text{-}Rh}) = 2900\ M^{-1}\ cm^{-1}$; $\epsilon^{350}(\mathbf{3\text{-}Rh}) = 2100\ M^{-1}\ cm^{-1}$) while the protein concentration was assayed either by the Bradford method or at 280 nm after subtraction of the contribution of the metal complex ($\epsilon^{280}(\mathbf{1\text{-}Rh}) = 20{,}500\ M^{-1}\ cm^{-1}$; $\epsilon^{280}(\mathbf{3\text{-}Rh}) = 3700\ M^{-1}\ cm^{-1}$). The Rh/P ratio (Table 1) for **cPAP-1-Rh** of 1.5 ± 0.25 was somehow surprising since the thiol/protein ratio is 0.75 for crude papain. Furthermore, since glycyl endopeptidase was shown not to react with **1-Rh**, the Rh/P for **cPAP-1-Rh** should be much below 0.75. This might indicate that aminoacids other than the active site cysteine are involved in the reaction with **1-Rh**.

The near-uv CD spectrum of bioconjugate **cPAP-1-Rh** displayed a significant increase of ellipticity around 260 nm with respect to **cPAP-NEM** prepared in the same conditions (Fig. S5). This increase may be due to intrinsic (change of environment around the aromatic residues of papain) or extrinsic factors.

Analysis of the metalloprotein resulting from the reaction of **afPAP** and **1-Rh** by LC-ESI–MS confirmed the formation of the bioconjugate as well as the presence of two other papain derivatives in the sample (Fig. S6). The value of 24,008 Da matched the calcu-

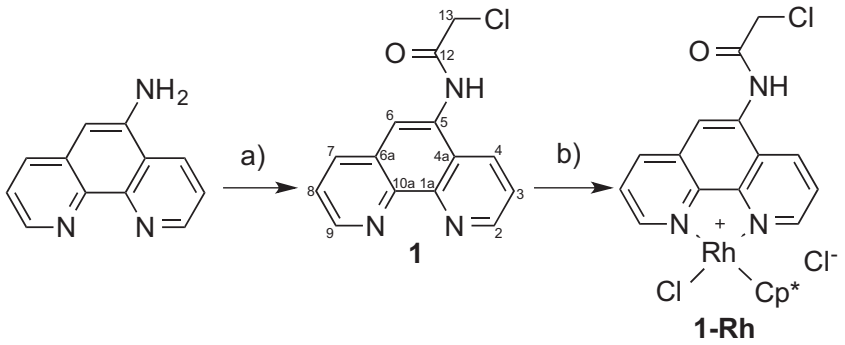

Scheme 1. (a) chloroacetyl chloride, TEA, DCM, −78 °C to RT, 93% ; (b) $[Cp^*Rh(\mu\text{-}Cl)Cl]_2$, DCM, RT, 36%.

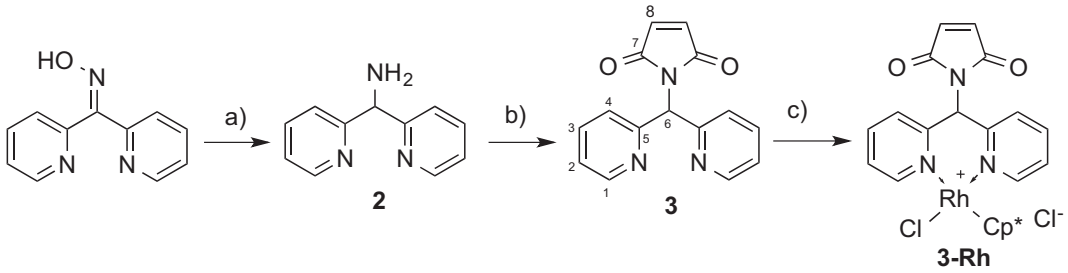

Scheme 2. (a) NH_4OAc, NH_4OH, Zn, H_2O/EtOH, Δ, 82%; (b) maleic anhydride, then $ZnCl_2$, HMDS, toluene, Δ, 74%; c) $[Cp^*Rh(\mu\text{-}Cl)Cl]_2$, DCM, RT, 96.

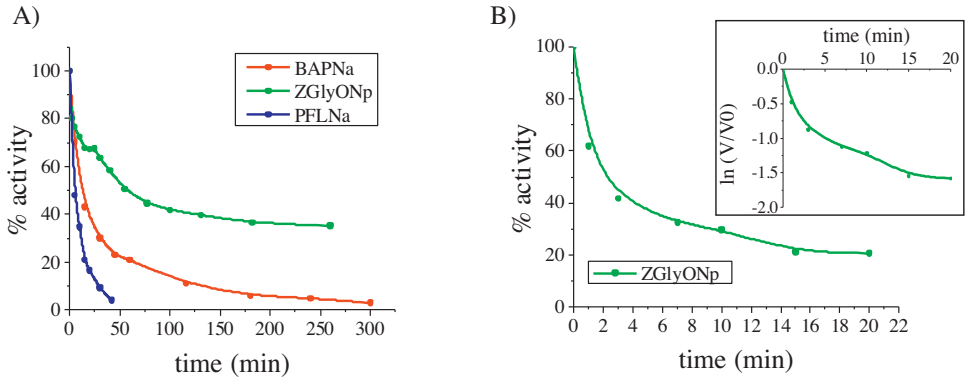

Fig. 1. (A) Time-dependent inactivation of crude papain (2 mg solid/ml in phosphate buffer pH 7; [thiol] = 110 μM) by **1-Rh** (1 mM). Hydrolytic activity periodically measured on BAPNa (red), PFLNa (blue) and ZGlyONp (green). (B) Time-dependent inactivation of gel filtered crude papain (0.093 mg/ml in PBS pH 7.4; [thiol] = 3 μM) by **3-Rh** (100 μM). Hydrolytic activity measured on ZGlyONp. Inset: semi-logarithmic plot of% hydrolysis rate vs. time. (For interpretation of the references to colour in this figure legend, the reader is referred to the web version of this article.)

lated mass of the species resulting from bioconjugation of **1-Rh** to papain via alkylation of the thiolate group of Cys25 and replacement of the chloro ligand by a trifluoroacetate ligand and allowed to rule out direct coordination of the Rh complex to sulphur (calculated MW = 23,930 Da) that may have occurred owing to rhodium thiophilicity. No peak corresponding to a double conjugate was observed on the mass spectrum, indicating that the rhodium content previously determined by absorption measurements had been severely overestimated.

3.3. Aqueous transfer hydrogenation of TFACP catalysed by the complexes and the metallopapains

Catalytic runs were carried out at the analytical scale on the activated ketone TFACP using Na formate as hydrogen donor (HD) (Scheme 3). Time course of the conversion to α-(trifluoromethyl) benzyl alcohol was monitored by HPLC (Fig. 2A). Quantitative conversion was reached in 1 h with **1-Rh** and 25 h with **3-Rh** at pH 7.4

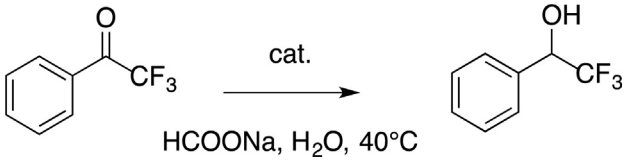

Scheme 3. Transfer hydrogenation of TFACP.

and 40 °C. Correlatively, the initial rate of conversion expressed as TOF was 3.5 times higher with **1-Rh** as compared to **3-Rh** (Table 2). Other aryl ketones were also reduced to the corresponding alcohols with good conversions in the presence of **1-Rh** (Table S1).

Since the (A)TH of ketones catalysed by analogous complexes is generally pH-dependent [42,46,49,82–84], we thought it relevant to carry out the catalytic runs at various pH. With **1-Rh**, conversion of TFACP was mostly independent of pH in the range between 3.4 and 8 (Fig. 3) as previously observed for the reduction of NAD^+

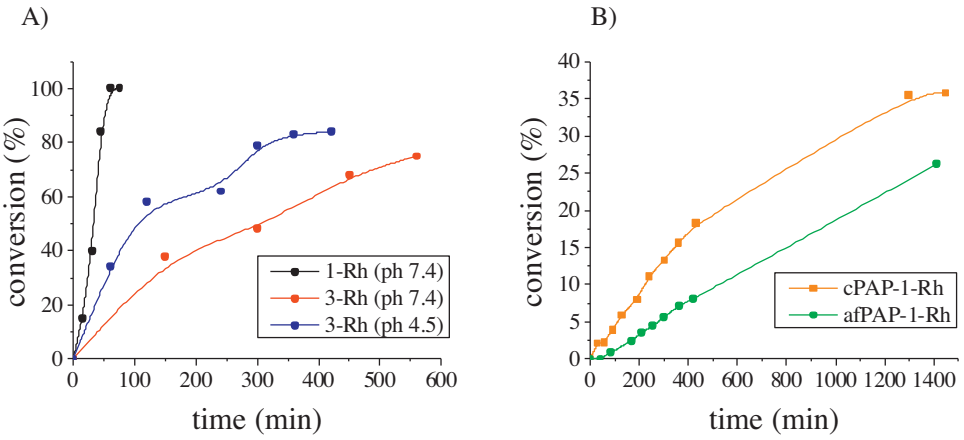

Fig. 2. (A) Time course of TH of TFACP in the presence of **1-Rh** or **3-Rh**. Conditions: [TFACP] = 10 mM, 1 mol% cat., [formate] = 1 M (pH 7.4 or 4.5), 40 °C. (B) Time course of TH of TFACP in the presence of **cPAP-1-Rh** or **afPAP-1-Rh**. Conditions: [TFACP] = 5 mM, 1 mol% cat., [formate] = 1 M in citrate-phosphate pH 5.1, 40 °C.

Table 2
(Asymmetric) transfer hydrogenation of TFACP catalyzed by **1-Rh**, **3-Rh** and the metallopapains. Conversion and ee determined by HPLC. Conditions: 1 mol% cat, 1 M formate pH 7.4, 40 °C.

Catalyst	TON (mol/mol)	TOF (h^{-1})	Conversion (%) [time, (h)]		ee (%)
1-Rh	100	56	100 [1.25][a]		–
3-Rh	94	16	95 [25][b]	86 [7][b,c]	–
cPAP-1-Rh	30	1.5	29 [24][b,d]		9 (S)[e]
afPAP-1-Rh	48	6	43 [24][b,d]		3 (S)
cPAP-3-Rh	20	–	16 [72][b,c]		5 (R)

[a] [TFACP] = 10 mM.
[b] [TFACP] = 5 mM.
[c] Citrate-phosphate pH 4.5.
[d] Citrate-phosphate pH 5.1.
[e] Determined by chiral GC.

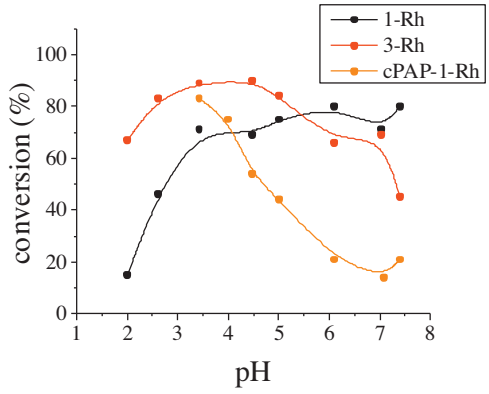

Fig. 3. Influence of pH on conversion of TFACP catalyzed by **1-Rh** (black), **3-Rh** (red) or **cPAP-1-Rh** (orange). Conditions: [TFACP] = 10 mM, 1 mol% cat, [formate] = 1 M, 30 min (**1-Rh**), 18 h (**3-Rh**) or 24 h (**cPAP-1-Rh**), 40 °C. (For interpretation of the references to colour in this figure legend, the reader is referred to the web version of this article.)

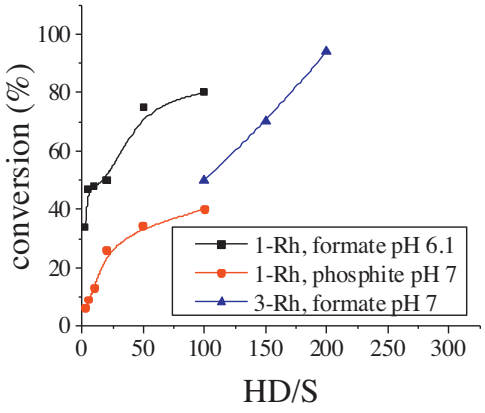

Fig. 4. Influence of hydrogen donor (HD) concentration on the conversion of TFACP catalyzed by **1-Rh** and **3-Rh**. Conditions: [TFACP] = 10 or 5 mM; 1 mol% cat, 30 min (**1-Rh**) or 24 h (**3-Rh**), 40 °C.

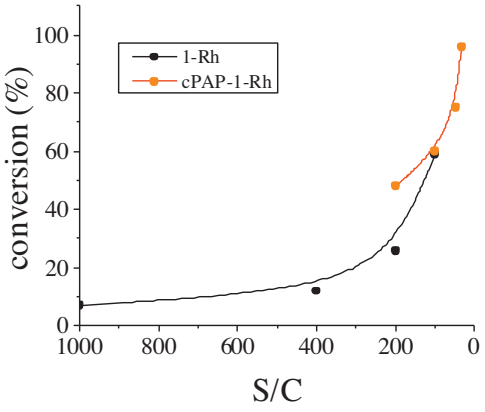

Fig. 5. Influence of catalyst load S/C on the conversion of TFACP catalyzed by **1-Rh** or **cPAP-1-Rh**. Conditions: [formate] = 1 M pH 6.1 (**1-Rh**) or pH 6.6 with phosphate buffer (**cPAP-1-Rh**), 30 min (**1-Rh**) or 24 h (**cPAP-1-Rh**), 40 °C.

catalysed by $[Cp^*Rh(bpy)(OH_2)]^{2+}$ [85]. With **3-Rh**, the optimal pH was found in the acidic range (between 3.4 and 5). Correlatively, the TOF increased from 16 h^{-1} at pH 7.4–38 h^{-1} at pH 4.5 (see Table 2).

The extent of conversion of TFACP by **1-Rh** and **3-Rh** at constant catalyst load was also found to increase with the concentration of formate (Fig. 4). Even with as low as 2.5 eq of formate with respect to substrate, conversion reached 34% in 30 min in the presence of **1-Rh**. Phosphite was found an alternative HD in the reduction of NAD^+ catalysed by $[Cp^*Rh(bpy)(OH_2)]^{2+}$ [86]. We found out that phosphite could act as hydrogen donor in the aqueous TH of TFACP catalysed by **1-Rh** but conversions were lower than with formate especially as low HD/S (Fig. 4). Conversions in the presence of **1-Rh** also increased with the catalyst load S/C, reaching 60% at 30 min with S/C = 100 (Fig. 5).

Gratifyingly, metallopapains **cPAP-1-Rh**, **afPAP-1-Rh** and **cPAP-3-Rh** were able to catalyse the TH of TFACP but at lower rates and conversions compared to the free complexes (Fig. 2B

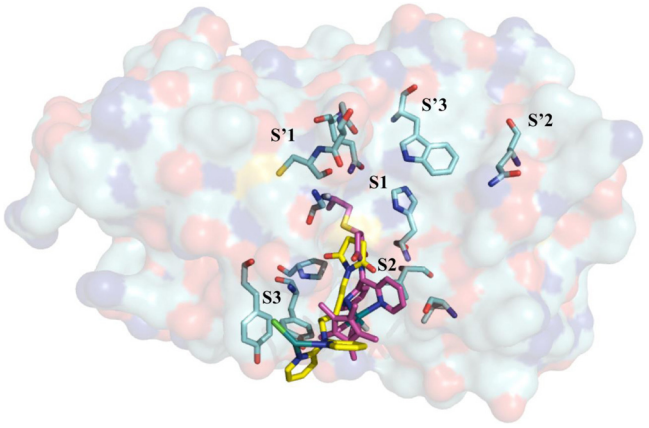

Fig. 6. Superimposition between the X-ray structure of papain covalently bound to an achiral Ru^{II} complex (PDB code: 4KP9) and the top-scoring pose of **3-Rh** obtained from covalent docking simulations. For the sake of clarity, only polar hydrogen atoms are displayed. Metal complexes and important residues are rendered as sticks while the protein is represented as a surface. Note that carbon atoms of the co-crystallized metal complex are rendered in yellow while those of the docked compound in magenta. (For interpretation of the references to colour in this figure legend, the reader is referred to the web version of this article.)

and Table 2). However, the ee's were disappointingly low, reaching at best 9% for **cPAP-1-Rh**. The catalytic activity of metallopapain **cPAP-1-Rh** followed a dramatically different trend as regards pH dependence (Fig. 4). The highest conversions were reached at acidic pH while conversion was the lowest around neutrality. This increase of conversion at acidic pH was accompanied with a nearly complete loss of enantioselectivity (ee <3% at pH 3.4). This behaviour is likely due to a change of conformation of the metalloenzyme as a function of pH that in turn influences the accessibility of the metal centre. Indeed, progressive unfolding of **cPAP-1-Rh** occurs at 40 °C in the presence of 1 M formate at pH 3.4 as shown by the progressive shift of the fluorescence emission from 331 to 344 nm within 19 h (not shown). Eventually, under optimal conditions of pH and S/C, full conversion of TFACP was reached within 24 h in the presence of 3.3 mol% **cPAP-1-Rh** (Fig. 6). A modest enantiomeric excess of 7–10% was obtained in favour of the (S)-enantiomer.

3.4. Theoretical insights

As above-mentioned, **1-Rh** and **3-Rh** were covalently anchored to the residue Cys25 within the papain active site. Schechter and Berger established that the binding site of papain contained 7 subsites, each one accommodating an aminoacid of the substrate [87]. These subsites were denominated from S1 to S4 (non-primed binding sites) and from S'1 to S'3 (primed binding sites). Later on, X-ray structural data on papain-inhibitor complexes brought to light the aminoacids involved in each subsite as follows: S1–Gln19, His159, Gly23; S2–Pro68, Val133, Val157; S3–Tyr61, Tyr67; S'1–Gly20, Ser21, Cys22; S'2–Gln142; S'3–Trp177.[88,89] These residues may establish additional non-covalent interactions with compounds bound to Cys25.

Fig. 6 shows the superimposition of the obtained top-scored pose of **3-Rh** and that taken from an X-ray solved structure of a similar metal complex bounded to papain having a Ru^{II} instead of Rh^{III} as metal (PDB code: 4KP9, resolution 2.10 Å [90]). Interestingly, the same subsites played similar roles and a good overlap was observed when superimposing docking and X-ray poses, thus suggesting that covalent docking is a valuable strategy for the present investigation. Furthermore, we observed that poses comparable to that obtained for **3-Rh** were also found for **1-Rh(R)** and **1-Rh(S)** compounds (see Fig. 7A). Importantly, both enantiomers were able to engage H-bond interactions with the backbones of Gly66 and Asp158 (Fig. 7C and Fig. 7D), while Tyr67 determined a distortion of the octahedral metal coordination because of steric hindrance only in case of **1-Rh(R)** enantiomer (Fig. 7B). On the contrary, H-bond interactions were not observed in the top-scored pose of **3-Rh** having a lower docking score (about 2 kcal/mol vs. 4 kcal/mol in both **1-Rh(R)** and **1-Rh(S)**). It is worth noting that the same H-bond interactions herein hypothesized for **1-Rh** have been observed in other X-ray solved covalent inhibitors of papain. Meaningful examples are given by benzyloxycarbonyl-glycyl-phenylalanyl-methylenylglycyl derivative (PDB code: 5PAD [76]) and L-leucyl-*N*-(2-oxopropyl)-L-phenylalaninamide (PDB code: 1KHQ [91]). On the basis of covalent docking simulations, we can thus derive that the higher enantioselective ability of **1-Rh** with respect to **3-Rh** is likely due to the different accessibility of the metal centre after covalent binding with papain. On one side, we observed that both **1-Rh** enantiomers could establish two H-bond interactions with the protein, having a stabilizing conformational effect. On the other, the lack of H-bond interactions allowed the **3-Rh** compound a higher conformation freedom, which impacted its enantioselectivity.

However, it is worth noting that the observed H-bond interactions involved only the amide group of **1-Rh** while, on the contrary, the metallic head was not able to establish any strong interaction with the protein residues, due to the absence of H-bond donors and/or acceptors substituents. This evidence not only offers a glimpse of a possible explanation of the observed low enantioselectivity but could pave the way for the design of new and more efficient piano-stool d^6-$rhodium^{III}$ complexes. This point is at the moment under investigation. Indeed, we are currently screening a large chemical library of polypyridine $rhodium^{III}$ complexes including various H-bond acceptors and donors bound to the metallic head.

4. Conclusions

Two half-sandwich polypyridine $rhodium^{III}$ complexes including a thiol-reactive function for covalent anchoring to papain were synthesized and characterized by usual spectroscopic means. Both were shown to inactivate papain in a time-dependent fashion by reaction with the native thiolate group of the active site cysteine, affording the expected biohybrid adducts. These inactivation experiments highlighted differences of reactivity of **1-Rh** and **3-Rh** towards the four homologous cysteine endoproteinases present in papaya latex and in particular the probable lack of inactivation of glycyl endopeptidase by **1-Rh**. Both complexes were shown to catalyse the aqueous transfer hydrogenation of an activated aryl ketone under mild conditions of temperature and pH with the phenanthroline complex being much more active than the bispyridine one. Covalent insertion of both metallic species within papain converted it to a transfer hydrogenase. Under optimized conditions of pH and catalyst load, conversion of TFACP was quantitative within 24 h in the presence of metallopapain **cPAP-1-Rh** and the alcohol product was obtained with a modest enantiomeric excess of 7–10% in favour of the (S)-enantiomer. Molecular modelling studies complemented the experimental data, giving a sound explanation to the lack of enantioselectivity of the hybrid catalysts. The agreement with experimental findings strongly supported the use of this theoretical approach combining quantum mechanics and covalent docking simulations when crystallographic data are not available. At present, we are screening a large chemical library of polypyridine $rhodium^{III}$ complexes with the aim to identify compounds having low conformational freedom after their covalent insertion within papain. We do believe that this ongoing attempt might help to address future design of more selective hybrid catalysis.

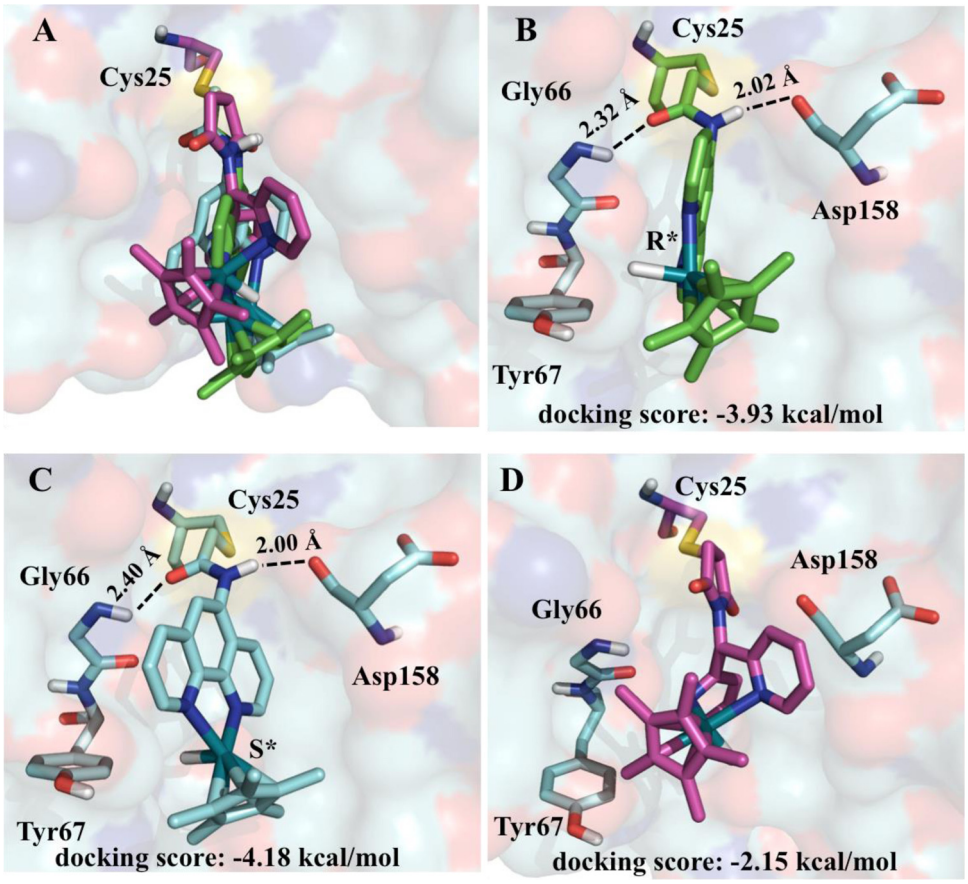

Fig. 7. Superimposition of the obtained top-scoring poses of **1-Rh(R)**, **1-Rh(S)** and **3-Rh**. (A); top scoring pose of **1-Rh(R)** (B); **1-Rh(S)** (C) and **3-Rh** (D). Ligands and important residues are rendered as sticks while protein is shown as a surface. H-bond interactions are depicted by a dotted line. For the sake of clarity, only the polar hydrogen atoms are displayed.

Acknowledgements

The Agence Nationale de la Recherche (ANR) is gratefully acknowledged for financial support (project "Artzymes", grant number ANR-11-BS07-027-01).This work was supported by the LabEx MiChem part of French state funds managed by the ANR within the Investissements d'Avenir programme under reference ANR-11-IDEX-0004-02. Part of this work was funded by the "Ville de Paris" under the program "Research in Paris 2014" (application number 200). Luca Signor (mass spectrometry platform, IBS, Grenoble, France) is gratefully acknowledged for ESI MS analyses.

Appendix A. Supplementary data

Supplementary data associated with this article can be found, in the online version, at http://dx.doi.org/10.1016/j.molcatb.2015.10.007.

References

[1] F. Rosati, G. Roelfes, ChemCatChem 2 (2010) 916–927.
[2] D.C.M. Albanese, N. Gaggero, RSC Adv. 5 (2015) 10588–10598.
[3] J.C. Lewis, ACS Catal. 3 (2013) 2954–2975.
[4] T. Heinisch, T.R. Ward, Curr. Opin. Chem. Biol. 14 (2010) 184–199.
[5] T.R. Ward, Acc. Chem. Res. 44 (2011) 47–57.
[6] P.J. Deuss, R. den Heeten, W. Laan, P.C.J. Kamer, Chem. Eur. J. 17 (2011) 4680–4698.
[7] H.-H. Otto, T. Schirmeister, Chem. Rev. 97 (1997) 133–171.
[8] A. El Moussaoui, M. Nijs, C. Paul, R. Wintjens, J. Vincentelli, M. Azarkan, Y. Looze, Cell. Mol. Life Sci. 58 (2001) 556–570.
[9] J. Drenth, J.N. Jansonius, R. Koekoek, B.G. Wolthers, Adv. Protein Chem. 25 (1971) 79–115.
[10] E. Shaw, Adv. Enzymol. Relat. Areas Mol. Biol. 63 (1990) 271–347.
[11] H.L. Levine, E.T. Kaiser, J. Am. Chem. Soc. 100 (1978) 7670–7677.
[12] H.L. Levine, E.T. Kaiser, J. Am. Chem. Soc. 102 (1980) 343–345.
[13] H.L. Levine, Y. Nakagawa, E.T. Kaiser, Biochem. Biophys. Res. Commun. 76 (1977) 64–70.
[14] J.T. Slama, S.R. Oruganti, E.T. Kaiser, J. Am. Chem. Soc. 103 (1981) 6211–6213.
[15] J.T. Slama, C. Radziejewski, S. Oruganti, E.T. Kaiser, J. Am. Chem. Soc. 106 (1984) 6778–6785.
[16] P. Haquette, B. Dumat, B. Talbi, S. Arbabi, J.-L. Renaud, G. Jaouen, M. Salmain, J. Organomet. Chem. 694 (2009) 937–941.
[17] P. Haquette, B. Talbi, S. Canaguier, S. Dagorne, C. Fosse, A. Martel, G. Jaouen, M. Salmain, Tetrahedron Lett. 49 (2008) 4670–4673.
[18] B. Talbi, P. Haquette, A. Martel, F. de Montigny, C. Fosse, S. Cordier, T. Roisnel, G. Jaouen, M. Salmain, Dalton Trans. 39 (2010) 5605–5607.
[19] L. Panella, J. Broos, J. Jin, M.W. Fraaije, D.B. Janssen, M. Jeromius-Stratingh, B.L. Feringa, A.J. Minnaard, J.G. de Vries, Chem. Commun. (2005) 5656–5658.
[20] M.T. Reetz, M. Rentzsch, A. Pletsch, M. Maywald, Chimia 56 (2002) 721–723.
[21] M.T. Reetz, M. Rentzsch, A. Pletsch, M. Maywald, P. Maiwald, J.J.-P. Peyralans, A. Maichele, Y. Fu, N. Jiao, F. Hollmann, R. Mondière, A. Taglieber, Tetrahedron 63 (2007) 6404–6414.
[22] N. Madern, B. Talbi, M. Salmain, Appl. Organomet. Chem. 27 (2013) 6–12.
[23] P. Haquette, B. Talbi, L. Barilleau, N. Madern, C. Fosse, M. Salmain, Org. Biomol. Chem. 9 (2011) 5720–5727.
[24] T. Reiner, D. Jantke, A.N. Marziale, A. Raba, J. Eppinger, ChemistryOpen 2 (2013) 50–54.
[25] R. Noyori, S. Hashiguchi, Acc. Chem. Res. 30 (1997) 97–102.
[26] J. Václavík, P. Kačer, M. Kuzma, L. Červený, Molecules 16 (2011) 5460–5495.
[27] J. Canivet, G. Labat, H. Stoeckli-Evans, G. Suss-Fink, Eur. J. Inorg. Chem. (2005) 4493–4500.
[28] J. Canivet, G. Suss-Fink, Green Chem. 9 (2007) 391–397.
[29] H.Y. Rhyoo, H.-J. Park, Y.K. Chung, Chem. Commun. (2001) 2064–2065.
[30] H.Y. Rhyoo, H.-J. Park, W.H. Suh, Y.K. Chung, Tetrahedron Lett. 43 (2002) 269–272.
[31] X. Wu, X. Li, W. Hems, J. Xiao, Org. Biomol. Chem. 2 (2004) 1818–1821.
[32] X. Wu, X. Li, F. King, J. Xiao, Angew. Chem. Int. Ed. 44 (2005) 3407–3411.
[33] X. Wu, X. Li, M. McConville, O. Saidi, J. Xiao, J. Mol. Catal. A: Chem. 247 (2006) 153–158.

[34] X. Wu, J. Liu, D. Di Tommaso, J.A. Iggo, C.R.A. Catlow, J. Basca, J. Xiao, Chem. Eur. J. 14 (2008) 7699–7715.
[35] X. Wu, D. Vinci, T. Ikariya, J. Xiao, Chem. Commun. (2005) 4447–4449.
[36] X. Wu, C. Wang, J. Xiao, Platinum Metals Rev. 54 (2010) 3–19.
[37] L. Li, J. Wu, F. Wang, J. Liao, H. Zhang, C. Lian, J. Zhu, J. Deng, Green Chem. 9 (2007) 23–25.
[38] N.A. Cortez, R. Rodriguez-Apodaca, G. Aguirre, M. Parra-Hake, T. Cole, R. Somanathan, Tetrahedron Lett. 47 (2006) 8515–8518.
[39] N.A. Cortez, G. Aguirre, M. Parra-Hake, R. Somanathan, Tetrahedron: Asymmetry 19 (2008) 1304–1309.
[40] D.J. Matharu, D.J. Morris, G.J. Clarkson, M. Wills, Chem. Commun. (2006) 3232–3234.
[41] D.S. Matharu, D.J. Morris, A.M. Kawamoto, G.J. Clarkson, M. Wills, Org. Lett. 7 (2005) 5489–5491.
[42] T. Abura, S. Ogo, Y. Watanabe, S. Fukuzumi, J. Am. Chem. Soc. 125 (2003) 4149–4154.
[43] J. Canivet, L. Karmazin-Brelot, G. Suss-Fink, J. Organomet. Chem. 690 (2005) 3202–3211.
[44] P. Govindaswamy, J. Canivet, B. Therrien, G. Suss-Fink, P. Stepnicka, J. Ludvik, J. Organomet. Chem. 692 (2007) 3664–3675.
[45] Y. Himeda, N. Onozawa-Kamatsuzaki, H. Sugihara, H. Arakawa, K. Kasuga, J. Mol. Cat. A: Chem. 195 (2003) 95–100.
[46] Y. Himeda, N. Onozawa-Komatsuzaki, S. Miyazawa, H. Sugihara, T. Hirose, K. Kasuga, Chem. Eur. J. 14 (2008) 11076–11081.
[47] C. Leiva, C. Lo, R.H. Fish, J. Organomet. Chem. 695 (2010) 145–150.
[48] I. Nieto, M.S. Livings, J.B.I. Sacci, L.E. Reuther, M. Zeller, E.T. Papish, Organometallics 30 (2011) 6339–6342.
[49] S. Ogo, T. Abura, Y. Watanabe, Organometallics 21 (2002) 2964–2969.
[50] S. Ogo, N. Makihara, Y. Kaneko, Y. Watanabe, Organometallics 20 (2001) 4903–4910.
[51] P. Stepnicka, J. Ludvik, J. Canivet, G. Suss-Fink, Inorg. Chim. Acta 359 (2006) 2369–2374.
[52] J.J. Soldevila-Barreda, P.C.A. Bruijnincx, A. Habtemariam, G.J. Clarkson, R.J. Deeth, P.J. Sadler, Organometallics 31 (2012) 5958–5967.
[53] M. Creus, A. Pordea, T. Rossel, A. Sardo, C. Letondor, A. Ivanova, I. Le Trong, R.E. Stenkamp, T.R. Ward, Angew. Chem. Int. Ed. 47 (2008) 1400–1404.
[54] M. Durrenberger, T. Heinisch, Y.M. Wilson, T. Rossel, E. Nogueira, L. Knorr, A. Mutschler, K. Kersten, M.J. Zimbron, J. Pierron, T. Schirmer, T.R. Ward, Angew. Chem. Int. Ed. 50 (2011) 3026–3029.
[55] C. Letondor, N. Humbert, T.R. Ward, Proc. Natl. Acad. Sci. U. S. A. 102 (2005) 4683–4887.
[56] C. Letondor, A. Pordea, N. Humbert, A. Ivanovna, S. Mazurek, M. Novic, T.R. Ward, J. Am. Chem. Soc. 128 (2006) 8320–8328.
[57] A. Pordea, M. Creus, C. Letondor, A. Ivanova, T.R. Ward, Inorg. Chim. Acta 363 (2010) 601–604.
[58] A. Chevalley, M.V. Cherrier, J.C. Fontecilla-Camps, M. Ghasemi, M. Salmain, Dalton Trans. 43 (2014) 5482–5489.
[59] A. Chevalley, M. Salmain, Chem. Commun. 48 (2012) 11984–11986.
[60] V. Muñoz Robles, E. Ortega-Carrasco, L. Alonso-Cotchico, J. Rodriguez-Guerra, A. Lledós, J.-D. Maréchal, ACS Catal. 5 (2015) 2469–2480.
[61] F.N. Castellano, J.D. Dattelbaum, J.R. Lakowicz, Anal. Biochem. 255 (1998) 165–170.
[62] M. Renz, C. Hemmert, B. Meunier, Eur. J. Org. Chem. (1998) 1271–1273.
[63] M.O. Funk, Y. Nakagawa, J. Skochdopole, E.T. Kaiser, Int. J. Peptide Protein Res. 13 (1979) 296–303.
[64] C. Riener, G. Kada, H. Gruber, Anal. Bioanal. Chem. 373 (2002) 266–276.
[65] W.D. Cornell, P. Cieplak, C.I. Bayly, P.A. Kollmann, J. Am. Chem. Soc 115 (1993) 9620–9631.
[66] A.D. Becke, J. Chem. Phys. 98 (1993) 5648–5652.
[67] M.J. Frisch, G.W., Trucks, H.B., Schlegel, G.E., Scuseria, M.A., Robb, J.R., Cheeseman, G., Scalmani, V., Barone, B., Mennucci, G.A., Petersson, H., Nakatsuji, M., Caricato, X., Li, H.P., Hratchian, A.F., Izmaylov, J., Bloino, G., Zheng, J.L., Sonnenberg, M., Hada, M., Ehara, K., Toyota, R., Fukuda, J., Hasegawa, M., Ishida, T., Nakajima, Y., Honda, O., Kitao, H., Nakai, T., Vreven, J.A.M. Jr., J.E. Peralta, F., Ogliaro, M., Bearpark, J.J., Heyd, E., Brothers, K.N., Kudin, V.N., Staroverov, R., Kobayashi, J., Normand, K., Raghavachari, A., Rendell, J.C., Burant, S.S., Iyengar, J., Tomasi, M., Cossi, N., Rega, N.J., Millam, M., Klene, J.E., Knox, J.B., Cross, V., Bakken, C., Adamo, J., Jaramillo, R., Gomperts, R.E., Stratmann, O., Yazyev, A.J., Austin, R., Cammi, C., Pomelli, J.W., Ochterski, R.L., Martin, K., Morokuma, V.G., Zakrzewski, G.A., Voth, P., Salvador, J.J., Dannenberg, S., Dapprich, A.D., Daniels, O., Farkas, J.B., Foresman, J.V., Ortiz, J., Cioslowski, D.J. Fox, in, Wallingford CT, 2009.
[68] J. Wang, W. Wang, P.A. Kollmann, D.A. Case, J. Mol. Graph. Model. 25 (2006) 247–260.
[69] D.A. Case, T.A., Darden, T.E.C., III, C.L., Simmerling, J., Wang, R.E., Duke, R., Luo, R.C., Walker, W., Zhang, K.M., Merz, B., Roberts, S., Hayik, A., Roitberg, G., Seabra, J., Swails, A.W. Götz, I. Kolossváíry, K.F., Wong, F., Paesani, J., Vanicek, R.M., Wolf, J., Liu, X., Wu, S.R., Brozell, T., Steinbrecher, H., Gohlke, Q., Cai, X., Ye, J., Wang, M.J., Hsieh, G., Cui, D.R., Roe, D.H., Mathews, M.G., Seetin, R. Salomon-Ferrer, C., Sagui, V., Babin, T., Luchko, S., Gusarov, A., Kovalenko, P.A. Kollman, in, University of California, San Francisco., 2012.
[70] I.G. Kamphuis, K.H. Kalk, M.B.A. Swarte, J. Drenth, J. Mol. Biol. 179 (1984) 233–256.
[71] Schrödinger Release 2014-4: Schrödinger Suite 2014-4, Protein Preparation Wizard LLC, New York, NY, 2014.
[72] Schrödinger Suite 2014-4, Schrödinger, LLC, New York, NY, 2014.
[73] Small-Molecule Drug Discovery Suite 2014-4: GLIDE, version 6.5, Schrödinger, LLC, New York, NY, 2014.
[74] J.L. Banks, H.S. Beard, Y. Cao, A.E. Cho, W. Damm, R. Farid, A.K. Felts, T.A. Halgren, D.T. Mainz, J.R. Maple, R. Murphy, D.M. Philipp, M.P. Repasky, L.Y. Zhang, B.J. Berne, R.A. Friesner, E. Gallicchio, R.M. Levy, J. Comput. Chem. 26 (2005) 1752–1780.
[75] P.Y. Reddy, S. Kondo, T. Toru, Y. Ueno, J. Org. Chem. 62 (1997) 2652–2654.
[76] J. Drenth, K.H. Kalk, H.M. Swen, Biochemistry 15 (1976) 3731–3738.
[77] K.T. Douglas, O.S. Ejim, K. Taylor, J. Enzyme Inhib. 6 (1992) 233–242.
[78] D.J. Buttle, Methods Enzymol. 244 (1994) 539–555.
[79] M. Azarkan, A. El Moussaoui, D. van Wuytswinkel, G. Dehon, Y. Looze, J. Chromatogr. B 790 (2003) 229–238.
[80] P.M. Dekeyser, S. De Smedt, J. Demeester, A. Lauwers, J. Chromatogr. B 656 (1994) 203–208.
[81] D.J. Buttle, A. Ritonja, P.M. Dando, M. Abrahamson, E.N. Shaw, P. Wikstrom, V. Turk, A.J. Barrett, FEBS Lett. 262 (1990) 58–60.
[82] X.F. Wu, X.H. Li, A. Zanotti-Gerosa, A. Pettman, J.K. Liu, A.J. Mills, J.L. Xiao, Chem. Eur. J. 14 (2008) 2209–2222.
[83] J. Canivet, G. Suss-Fink, P. Stepnicka, Eur. J. Inorg. Chem. (2007) 4736–4742.
[84] C. Romain, S. Gaillard, M.K. Elmkaddem, L. Toupet, C. Fischmeister, C.M. Thomas, J.-L. Renaud, Organometallics 29 (2010) 1992–1995.
[85] F. Hollmann, B. Witholt, A. Schmid, J. Mol. Catal.: B 19–20 (2003) 167–176.
[86] M. Mifsud Grau, M. Poizat, I.W.C.E. Arends, F. Hollmann, Appl. Organomet. Chem. 24 (2010) 380–385.
[87] I. Schechter, A. Berger, Biochem. Biophys. Res. Commun. 27 (1967) 157–162.
[88] J.M. LaLonde, B. Zhao, W.W. Smith, C.A. Janson, R.L. DesJarlais, T.A. Tomaszek, T.J. Carr, S.K. Thompson, H.-J. Oh, D.S. Yamashita, D.F. Veber, S.S. Abdel-Meguid, J. Med. Chem. 41 (1998) 4567–4576.
[89] D. Turk, G. Guncar, M. Podobnik, B. Turk, Biol. Chem. 379 (1998) 137–147.
[90] M.V. Cherrier, N. Madern, P. Amara, M. Salmain, J.C. Fontecilla-Camps, 10.2210/pdb4kp9/pdb (2013).
[91] R. Janowski, E. Kozak, E. Jankowska, Z. Grzonka, M. Jaskolski, J. Pept. Res. 64 (2004) 141–150.